An ab initio study of methane activation on lanthanide oxide

Chak-Tong Au [a], Tai-Jin Zhou [a,b], Wu-Jiang Lai [a,b] and Ching-Fai Ng [a]

[a] *Department of Chemistry, Hong Kong Baptist University, Kowloon, Hong Kong*
[b] *Department of Chemistry, Xiamen University, Xiamen 361005, PR China*

Received 7 July 1997; accepted 2 October 1997

Ab initio MP2 calculations have been carried out to study the activation of methane on lanthanide oxide La_2O_3. O^- and O_2^{2-} are assumed to be the active species on the oxide surface. The possible roles of O^{2-} and O_2^{4-} on the oxide surface in C–H bond activation are also investigated. It is shown that the CH_4 oxidative dehydrogenation occurs much more readily on O^- and O_2^{2-} than on O^{2-} and O_2^{4-}. The results indicate that O^- and O_2^{2-} are the active species and therefore support the O^- and O_2^{2-} mechanisms assumed for the reactions. The promoter compound containing Br^- is found to be favorable for the methane activation.

Keywords: ab initio calculations, OCM reaction, La_2O_3, carbene, O^-, O_2^{2-}

1. Introduction

There has been a plethora of experimental investigation on the oxidative coupling of methane (OCM) on metal oxide surfaces as the process has considerable significance in the utilization of natural gas. The OCM topic has been reviewed by Hutchings et al. [1], Anderson [2], Amenomiya et al. [3], Maitra [4], Krylov [5], and others. From these review articles, one can realize that the compounds adopted in effective catalysts for the reaction are largely rare earth, alkali and alkaline earth oxides. Of particular importance are the oxides of lithium, magnesium, barium and lanthanum.

Different mechanisms have been suggested for the OCM reaction. One mechanism is based on O^- as the active site. According to this mechanism, O^- species occurring on oxide surfaces initiate the catalytic process by abstracting a hydrogen atom from methane, forming an OH^- group and a methyl radical. The formation of methyl radicals in the gas-phase has been confirmed experimentally [6]. Theoretical support for this mechanism has been given by Anderson and co-workers, who carried out calculations on cluster models of the MoO_3 [7], $CuMoO_4$ [8] and MgO [9] oxide structures and found that O^- strongly activates the C–H bonds. Many experimental studies of OCM have also shown that O^- centers on oxide surfaces possess the ability of cleaving the CH bonds (e.g. [6,10–12]). Another mechanism is based on O^{2-} with a low coordinate number. The latter views the catalyst's primary role is to abstract hydrogen from methane in an acid–base reaction [3].

There have been a number of theoretical studies of hydrogen abstraction from methane on MgO [9,13–18]. MgO is one of the catalysts extensively studied experimentally. Theoretical studies of methane activation on other metal oxides are very rare [7,8,14,17–20]. In this paper we attempt to perform an ab initio study of methane activation on La_2O_3. Earlier, we reported the performance of LaF_3/La_2O_3 catalysts [21]. They are active in the conversion of CH_4 to C_2H_6. In our recent studies of the process over La_2O_3 catalysts promoted by barium and bromine [22], we found that LaOBr and $BaCO_3/LaOBr$ catalysts can give a high C_2H_4/C_2H_6 ratio. In situ Raman experiments showed that the catalysts were capable of forming O_2^{2-} species during OCM reaction while the results of the CH_4/CD_4 (1 : 1) experiments suggested that carbene was an active intermediate participating in the formation of C_2H_4. Based on these results, we proposed O_2^{2-} as the active species which can abstract two hydrogen atoms from CH_4 simultaneously to produce carbene and the carbenes generated would couple to give C_2H_4. The roles of Br^- and Ba^{2+} were to promote the generation of O_2^{2-} on the surfaces of the catalysts as well as to stabilize them at OCM reaction temperatures. The aim of the present work is to compare the feasibility of hydrogen abstraction from CH_4 by O^-, O_2^{2-}, O^{2-} and O_2^{4-} on La_2O_3 based on the high-level ab initio quantum chemistry method.

2. Computational details

2.1. Computational method

The GAUSSIAN 94 program package [23] has been used for all calculations. The core electrons, i.e. [Xe] for La, were fitted to the effective core potentials of Hay and Wadt [24], in which the relativistic mass–velocity effect and Darwin effect were included. The valence electrons of all atoms were described with the standard Lan2DZ basis sets, D95 for O (721/41), C (721/41), H (31) and DZ for La (341/321/21). The second-order Møller–Plesset perturbation was used to treat correlation effects. Different levels of approximation were also tested for

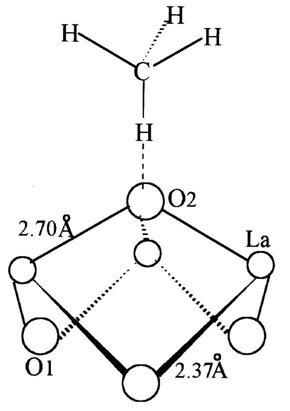

Figure 1. The geometry of the $[La_3O_4]^{2+}CH_4$ cluster which was used to model the activation of CH_4 and La_2O_3.

some small systems. The geometries of molecular structures (containing both equilibrium and transition states) were obtained according to the Berny geometry optimization algorithm [25].

2.2. Surface modeling

La_2O_3 belongs to the hexagonal structure, space group P$\bar{3}$m1 [26]. We used a 7 atom cluster model consisting of 3 lanthanum cations and 4 oxygen anions for the calculations. The cluster carries a formal charge of 1+. The model used for the CH_4 activation on the surface is shown in figure 1. In order to model a surface O^-, we removed an electron from the cluster. The molecular part above the surface was fully optimized under the constraint of C_{3v} symmetry. The calculations were also carried out with the simplest diatomic La^{3+}–O^- model. A linear O^{2-}–La^{3+}–O^- cluster was also examined. This model is used to simulate the activation of methane by O^- species adsorbed on La_2O_3. The La–La and La–O distances are based on La_2O_3 crystal structure data [26] (see figure 1).

In order to model the interaction of CH_4 with O_2^{2-} for the LaOBr catalyst which promotes carbene mechanism [22], a La^{3+}–O^-–O^-–La^{3+} model is used. The O^-–O^- species abstracts two H atoms from CH_4 simulta-

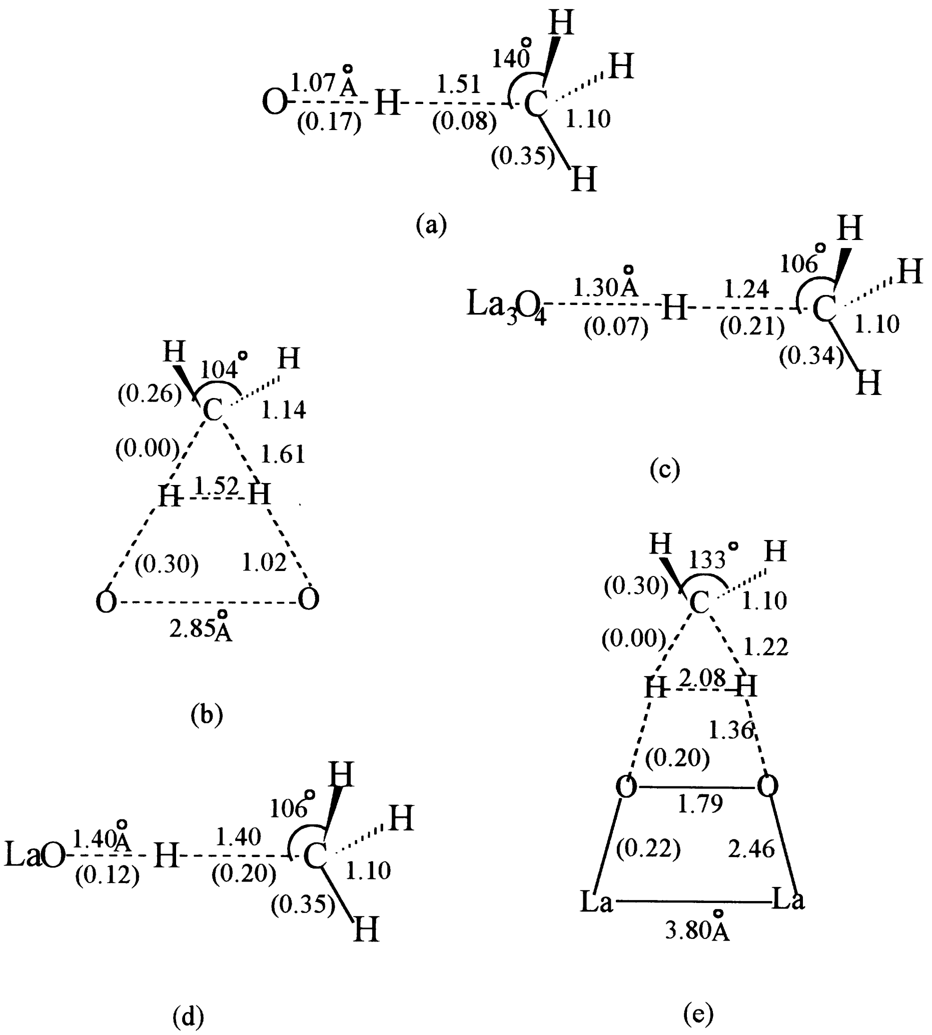

Figure 2. Calculated bond lengths, bond angles and bond orders (data in brackets) at transition state.

Table 1
Calculated results[a] for O_2^{2-} and the reaction $O_2^{2-} \rightarrow O^- + O^-$ at different levels of approximation (TS = transition state)

Method	R_e	R^{TS}	D_e	E_a
HF	1.60	4.47	−175	76.0
MP2	1.75	2.36	−117	7.4
QCISD	1.77	2.26	−125	3.4
exp. [b]			−104	

[a] Bond length R in Å, dissociation energy D_e and activation energy E_a in kcal/mol.

[b] Experimental value is from ref. [29].

neously (see figure 2e). For computational convenience, we have neglected Br^- in the calculations. The optimization was done under the constraint of C_{2v}.

3. Results and discussion

3.1. Performance of methods

In order to justify the use of the MP2 method for the following reaction systems, some test calculations have been carried out. Table 1 shows the results for the O_2^{2-} properties (bond length, dissociation energy, activation energy for $O_2^{2-} \rightarrow O^- + O^-$) calculated at the HF, MP2 and QCISD levels of approximation and table 2 shows the calculated reaction energies for $CH_2 + CH_2 \rightarrow C_2H_4$, $CH_4 + O_2^{2-} \rightarrow CH_2 + 2OH^-$ and $CH_4 + O^- \rightarrow CH_3 + OH^-$ at these levels. Apparently, MP2 and QCISD methods lead to close results. There are large discrepancies between the HF results and the results obtained by MP2 or QCISD method. Hence, it is necessary to include electron correlation in order to obtain reliable data.

Table 3 gives the calculated properties of isolated CH_x ($x = 4, 3, 2, 1$) and OH at the MP2 level, together with experimental data [27]. The calculated bond lengths and bond angles are shown to be close to the experimental values. The calculated dissociation energies ($CH_x \rightarrow CH_{x-1} + H$) compare in most cases favorably with the experimental ones. A relatively large discrepancy is found for the dissociation energy of CH, the error being 27 kcal/mol.

We also report the results of MP2 calculations on methane activation over diatomic MgO, LiO and AlO entities since there exist some accurate CI calculations in the literature [14]. Table 4 shows that for MgO and LiO, the MP2 results are quite close to the results obtained by Børve and Petterson [14] using the CCI+Q method. AlO is exceptional: the MP2 calculation gives significantly lower activation energy and reaction energy than the CCI+Q calculation.

Table 2
Calculated reaction energies (kcal/mol) at different levels of approximation

Reaction	HF	MP2	QCISD
$CH_2 + CH_2 \rightarrow C_2H_4$	−114	−163	−165
$CH_4 + O_2^{2-} \rightarrow CH_2 + 2OH^-$	−129	−92	−79
$CH_4 + O^- \rightarrow CH_3 + OH^-$	23	10	12

Table 3
Molecular properties[a] of the CH_x ($x = 4, 3, 2, 1$) and OH^- species calculated based on the MP2 method. Available experimental data[b] are included for comparison

Species	$2S+1$	R_{CH}^{calc}	R_{CH}^{exp}	$\angle_{HCH}^{calc}$	$\angle_{HCH}^{exp}$	D_e^{calc}	D_e^{exp}
CH_3–H (T_d)	1	1.08	1.086			97.1	103.3
CH_2–H (D_{3h})	2	1.09	1.079			105.0	109.6
CH–H	1	1.08	1.111	105.2	102.4	77.7	90.7
CH–H	3	1.08	1.078	180	136.0	100.3	99.7
C–H	4	1.14	1.120			107.1	79.9
O–H	2	1.00	0.971			78.9	101.3

[a] Bond length R in Å, angle ($\angle$) in degree and dissociation energy D_e in kcal/mol.

[b] Experimental data are those cited in ref. [27].

Since QCISD calculations are very time-consuming and the MP2 level of approximation appears to be satisfactory, we perform our calculations based only on the MP2 methods.

3.2. Hydrogen abstraction from methane by O^- and O_2^{2-}

For the sake of comparison, the reactions of CH_4 with isolated O^- and O_2^{2-} species are also of interest. The results are given in table 5.

The reaction $CH_4 + O^- \rightarrow CH_3 + OH^-$ is endothermic by 9.7 kcal/mol. The barrier height to the abstraction reaction is calculated to 13.1 kcal/mol. The relatively low activation energy suggests that the abstraction of one H atom from CH_4 by O^- is easy. Based on the OH and CH bond lengths and the Mulliken bond orders shown in figure 2a, one can see that in the transition state (TS) the CH bond is nearly broken while the OH bond is approximately formed (the C–H bond order decreases from 0.35 to 0.08 and the O–H bond

Table 4
Comparison of the calculated results[a] for the abstraction reaction, $MO + CH_4 \rightarrow MOH + CH_3$, between the MP2 and CCI+Q[b] levels (TS = transition state)

		R_{O-H}^{TS}	R_{C-H}^{TS}	$\angle_{HCH}^{TS}$	E_a	D_e
LiO	MP2	1.30	1.21	106.9	13.2	−15.7
	CCI+Q[b]	1.35	1.21	106.8	13.0	−14.2
MgO	MP2	1.31	1.21	105.9	12.4	−12.6
	CCI+Q[b]	1.31	1.22	107	9.2	−11.8
AlO	MP2	1.42	1.18	107.4	2.7	−24.8
	CCI+Q[b]	1.33	1.21	107	12.8	−9.7
BaO	MP2	1.20	1.33	107.0	4.1	−154.0

[a] Bond length R in Å, angle ($\angle$) in degree, activation energy E_a and reaction energy D_e in kcal/mol.

[b] From ref. [14].

Table 5
Calculated results[a] for the abstraction of H from CH_4 on various models (TS = transition state)

	R^{TS}_{La-O}	R^{TS}_{O-H}	R^{TS}_{C-H}	$\angle^{TS}_{HCH}$	E_a	D_e
O^-		1.07	1.51	104	13.1	9.7
O_2^{2-}		1.02	1.61	104	10.3	−92.0
$(O^{2-})_3(La^{3+})_3O^-$		1.30	1.24	106	15.0	−11.2
$(O^{2-})_3(La^{3+})_3O^{2-}$					–[b]	65.3
$La^{3+}O^-$		1.40	1.40	99	16.9	−25.2
$La^{3+}O^{2-}$		1.10	1.6	105	66.5	42.7
$La^{3+}O^-$	2.05[c]	1.70	1.36	99	8.3	−50.9
$La^{3+}O^{2-}$	2.14[c]	1.66	1.13	108	82.9	55.2
$O^{2-}La^{3+}O^-$	2.32[c]	1.27	1.25	107	1.6	−20.5
$Br^-La^{3+}O^-$		1.40	1.35	101	0	−31.1
$Br^-La^{3+}O^{2-}$		1.10	1.34	109	54.6	48.9
$(La^{3+})_2(O^-)_2$		1.36	1.22	133	28.6	−107.0
$(La^{3+})_2(O^{2-})_2$					–[b]	57.5

[a] Bond length R in Å, angle (∠) in degree, activation energy E_a and reaction energy D_e in kcal/mol.

[b] The activation energies were not obtained.

[c] The La–O distance is allowed to relax during geometry optimization.

order increases from 0 to 0.17). The overall abstraction reaction conserves the number of bonds in the system.

In the case of O_2^{2-}, the reaction $CH_4 + O_2^{2-} \rightarrow CH_2 + 2OH^-$ is strongly exothermic (by 92 kcal/mol). The activation energy is determined to be 10.3 kcal/mol, which is slightly lower than the activation energy for the $CH_4 + O^- \rightarrow CH_3 + OH^-$ reaction. According to the O_2^{2-} model, two equivalent C···H···O three-center bonds are formed simultaneously in TS. Comparing figure 2a with figure 2b, one can see that in the transition state the C–H bond length to oxygen is 0.1 Å larger in the latter system than in the former one. Another difference between figure 2a and figure 2b is that in figure 2b the abstraction reaction does not conserve the bonds. In the $CH_4 + O_2^{2-}$ reaction, the number of broken bonds is three (two C–H and one O–O) and the number of formed bonds is two (two O–H).

3.3. *Methane dehydrogenation over $[La_3O_4]^{2+}$, $[LaO]^{2+}$ and $[La_2O_2]^{4+}$*

The optimized transition state (TS) geometries for the CH_4 interaction on the $[La_3O_4]^{2+}$, $[LaO]^{2+}$ and $[La_2O_2]^{4+}$ models are shown in figures 2c–2e, respectively. In order to examine the nature of the bonding in the TS, the Mulliken bond orders for O–H and C–H are also given in the figures (values in parentheses). We have also explored the possible role of O^{2-} and O_2^{4-} sites on the oxide surface in C–H bond activation. Therefore we have tested the corresponding $[La_3O_4]^+$, $[LaO]^+$ and $[La_2O_2]^{2+}$ models with La and O in their normal oxidation states of 3+ and 2−, respectively. The calculated results on the various models are collected in table 5.

The calculations yield an activation energy of 15.0 kcal/mol for H abstraction from CH_4 on the $[La_3O_4]^{2+}$ model. The reaction energy D_e is calculated as −11 kcal/mol. The HOMO of this model, $5a_1$, is partially occupied and can accept an electron from the C–H antibonding orbital. Therefore the reaction $CH_4 + [La_3O_4]^{2+}$ is feasible and requires a relatively low activation energy. In the TS (figure 2c), the H_3C–H bond length and bond order vary insignificantly. This is in contrast to the O^- case (figure 2a). We see that here the O–H bond length is considerably larger than in O^-HCH_3. This can be understood by examining the models. The positive ion model has strong electrophilic character and the negative ion model has strong nucleophilic character. When CH_4 approaches from far distance to the positive ion, the electron in the C–H bond is removed to the half-filled HOMO of $[La_3O_4]^{2+}$ before the breaking of the C–H bond. It is the other way round with the negative ion model. Consequently, the O–H bond length in the TS is larger for the positive ion model than for the negative ion model. A calculation for the $[La_3O_4]^+$ model gives a very positive reaction energy. We have not obtained an activation energy for this model. The calculated high endothermicity of the reaction may indicate that the activation energy would be high. $[La_3O_4]^+$ is a closed-shell system, i.e. its HOMO is now completely filled. The LUMO is mainly La 6s in character (see table 6).

With the use of a minimal $[LaO]^{2+}$ model, the calculated energy barrier is 16.9 kcal/mol, which is similar to the calculated value on the larger cluster. The HOMO of $[LaO]^{2+}$ is partially occupied, similar to the $[La_3O_4]^{2+}$ case. For this model, we have also performed a calculation with the La–O bond length being relaxed during the search of TS and found an activation energy of 8 kcal/mol in this case. For $[LaO]^+$ with fully occupied HOMO, the calculation produces a high activation energy (67 kcal/mol) and a rather positive reaction energy (43 kcal/mol). For a calculation where the La–O distance is allowed to relax, an even higher activation energy (83 kcal/mol) is obtained.

Table 6
Calculated gross Mulliken populations and atomic charges. The main atomic composition of HOMO and LUMO are given

Species	La 5d	La 6s	O 2s	O 2p	Q_O	HOMO	LUMO
O^-			2.00	5.00	−1.00	$2p^5$	$3s^0$
$(O^-)_2$			1.96	5.04	−1.00	$1\pi_g^4$ (O 2p)	$2\sigma_u^0$ (O $2p_z$)
$[La_3O_4]^{2+}$	0.80	0.11	1.95	4.78	−0.72	$5a_1^1$ (O 2p)	$6a_1^0$ (La 6s)
$La^{3+}O^-$	0.52	0.01	1.98	4.43	−0.41	$1\pi^3$ (La 5d + O 2p)	$3\sigma^0$ (La 6s)
$(La^{3+})_2(O^-)_2$	0.06	0.53	1.97	4.42	−0.39	$1a_2^2$ (La 5d + O 2p)	$2b_1^0$ (La 5d)
$(La^{3+})_2(O^{2-})_2$	1.32	0.00	1.94	4.66	−0.60	$2b_1^2$ (La 5d)	$4a_1^0$ (La 6s)

For the interaction of CH_4 with $[La_2O_2]^{4+}$, the calculation yields an activation energy of about 29 kcal/mol (for this model, the O–O distance has been allowed to relax during the geometry optimization). The reaction process is highly exothermic. Table 6 shows that the HOMO of this model ($1a_2$) is fully occupied. Nevertheless, the barrier is quite low. This implies that (two) electrons from the (two) C–H bonds can easily be transferred to the LUMO $2b_1$, which mainly consists of La 5d. For $[La_2O_2]^{2+}$, the $2b_1$ orbital is now fully filled and the calculated reaction energy is greatly endothermic (also an activation energy has not been obtained for this model).

From the Mulliken population analysis in table 6, the most notable feature here is that the character of the "frontier" MO (HOMO or LUMO) of the model plays an important role in activating CH_4. For $[La_3O_4]^{2+}$ and $[LaO]^{2+}$, the HOMOs are partially occupied and therefore constitute the frontier MOs; for $[La_2O_2]^{4+}$ the LUMO is the frontier MO. These MOs happen to be made up of either O 2p, La 5d or the mixing of both. For $[La_3O_4]^+$, $[LaO]^+$ and $[La_2O_2]^{2+}$, the frontier MOs are the LUMOs which are mainly composed of La 6s. Therefore O 2p and La 5d are more effective than La 6s for the activation of CH_4. Anderson and co-workers [28] pointed out that the reason for the high activity of O^- in methane dehydrogenation is that $O^-_{(ads)}$ can provide a low-lying half-filled orbital that can take one electron from the CH–O σ^*-antibonding orbital during the CH bond breaking and OH bond processes; the low activity of O^{2-} in methane dehydrogenation was ascribed to the "four-electron closed-shell repulsion" between O^{2-} and CH_4. These arguments are in principle consistent with ours. If there are low-lying empty orbitals on the surface which can accept an electron (as in the case of Bi_2O_3 [20]), the reaction $CH_4 + O^{2-}_{(ads)} \rightarrow CH_3 + OH_{(ads)} + e$ is feasible.

For a $O^{2-}La^{3+}O^-$ model, an activation energy of 1.6 kcal/mol is obtained. This means that the O^- species adsorbed on the oxide surface are highly reactive. When the $[LaO]^+$ model is terminated by a Br^- ion, the calculated activation energy is decreased by 12 kcal/mol (as compared with that calculated on $[LaO]^+$).

4. Conclusions

Methane activation on the lanthanide oxide La_2O_3 has been studied by means of the ab initio MP2 method. Different models were used to simulate the bulk oxide. We have calculated reaction energetics of the C–H bond activation by O^-, O_2^{2-}, O^{2-} and O_2^{4-} for sites on the oxide surface. The abstractions of hydrogen from methane by O^- and O_2^{2-} are found to proceed with low activation energies E_a and the calculated reaction energies D_e are exothermic. The calculations based on the O^{2-} and O_2^{4-} models give remarkably higher E_a's and rather positive D_e's. Therefore, O^{2-} and O_2^{4-} on the oxide surface are unreactive towards hydrogen abstraction. This supports the O^- and O_2^{2-} mechanisms assumed for the reactions and is also in agreement with some experimental evidence indicating O^- as the reaction site [6,10–12]. We find that the calculated energetics depend on the electronic structure of the model: The character of the "frontier" MO (HOMO or LUMO) of the model plays an important role in activating CH_4. For the O^- and O_2^{2-} models, the frontier MO consists of O 2p or La 5d. For the O^{2-} and O_2^{4-} models, the frontier MO is mainly composed of La 6s. Thus, O 2p and La 5d are more reactive than La 6s for the activation of CH_4. The presence of Br^- in the promoter compound is found to be beneficial to the methane activation.

Acknowledgement

This work was supported by the Faculty Research Grant (FRG/94-95/II-53) of the Hong Kong Baptist University and the National Natural Science Foundation of China.

References

[1] G.J. Hutchings, M.S. Scurrel and J.R. Woodhouse, Chem. Soc. Rev. 18 (1989) 251.
[2] J.R. Anderson, Appl. Catal. 47 (1989) 177.
[3] Y. Amenomiya, V.I. Birss, M. Goledzinowski, J. Galuska and A.R. Sanger, Catal. Rev. Sci. Eng. 32 (1990) 163.
[4] A.M. Maitra, Appl. Catal. A 104 (1993) 11.
[5] O.V. Krylov, Catal. Today 18 (1993) 209.
[6] D.J. Driscoll, W. Martir, J.-X. Wang and J.H. Lunsford, J. Am. Chem. Soc. 107 (1985) 58.
[7] S.P. Mehandru, A.B. Anderson, J.F. Brazdil and R.K. Grasselli, J. Phys. Chem. 91 (1987) 2930.
[8] M.D. Ward, J.F. Brazdil, S.P. Mehandru and A.B. Anderson, J. Phys. Chem. 91 (1987) 6515.
[9] S.P. Mehandru, A.B. Anderson and J.F. Brazdil, J. Am. Chem. Soc. 110 (1988) 1715.
[10] T. Ito, J.-X. Wang, C.-H. Lin and J.H. Lunsford, J. Am. Chem. Soc. 107 (1985) 5062.
[11] T. Ito and J.H. Lunsford, Nature 314 (1985) 721.
[12] D.J. Driscoll and J.H. Lunsford, J. Phys. Chem. 89 (1985) 4415.
[13] C.M. Zicovich-Wilson, R. Gonzalez-Luque and P.M. Viruela-Martin, J. Mol. Struct. THEOCHEM 208 (1990) 153.
[14] K.J. Børve and L.G.M. Pettersson, J. Phys. Chem. 95 (1991) 3214.
[15] K.J. Børve and L.G.M. Pettersson, J. Phys. Chem. 95 (1991) 7401.
[16] K.J. Børve, J. Chem. Phys. 95 (1991) 4626.
[17] D.S. Maria-Aglaia, C. Athanasios, A.T. Constantinos and E.X. Constantinos, J. Mol. Catal. 82 (1993) 425.
[18] Y. Aray, J. Rodriguez, J. Murgich and F. Ruette, J. Phys. Chem. 97 (1993) 8393.
[19] M.J. Capitán, J.A. Odriozola, A. Márquez and J.F. Sanz, J. Catal. 156 (1995) 273.
[20] S.P. Mehandru, A.B. Anderson and J.F. Brazdil, J. Chem. Soc. Faraday Trans. I 83 (1987) 463.
[21] C.-T. Au, Y.-Q. Zhang, C.-F. Ng and H.-L. Wan, Catal. Lett. 23 (1994) 37.

[22] C.-T. Au, H. He, S.-Y. Lai and C.-F. Ng, J. Catal. 163 (1996) 399.

[23] M.J. Frisch, G.W. Trucks, H.B. Schlegel, P.M.W. Gill, B.G. Johnson, M.A. Robb, J.R. Cheeseman, T. Keith, G.A. Petersson, J.A. Montgomery, K. Raghavachari, M.A. Al-Laham, V.G. Zakrzewski, J.V. Ortiz, J.B. Foresman, C.Y. Peng, P.Y. Ayala, W. Chen, M.W. Wong, J.L. Andres, E.S. Replogle, R. Gomperts, R.L. Martin, D.J. Fox, J.S. Binkley, D.J. Defrees, J. Baker, J.P. Stewart, M. Head-Gordon, C. Gonzalez and J.A. Pople, GAUSSIAN 94, Revision B.2 (Gaussian Inc., Pittsburgh, 1995).

[24] P.J. Hay and W.R. Wadt, J. Chem. Phys. 82 (1985) 270.

[25] H.B. Schlegel, J. Comp. Chem. 3 (1982) 214.

[26] O. Greis, J. Solid State Chem. 34 (1980) 39.

[27] B.G. Johnson, P.M.W. Gill and J.A. Pople, J. Chem. Phys. 98 (1993) 5612.

[28] J.W. Yu and A.B. Anderson, J. Am. Chem. Soc. 112 (1990) 7218.

[29] A. Bielanńsk and J. Haber, *Oxygen in Catalysis* (Dekker, New York, 1991).